Influence of Reaction Times and Anticipation on Stability of Vehicular Traffic Flow

Martin Treiber, Arne Kesting, and Dirk Helbing

Two causes for the instability of traffic flow are investigated: the time lag caused by finite accelerations of vehicles and the delay caused by finite reaction times of drivers. Furthermore, the degree to which drivers may compensate for these delays is simulated by looking several vehicles ahead and anticipating future traffic situations. Since vehicular traffic flow is an extended multiparticle system with many degrees of freedom, two concepts of linear stability have to be considered: (*a*) local stability of a car following a leader that drives at constant velocity and (*b*) string (chain) stability of a platoon of several vehicles following each other. Typically, string stability is a much more restrictive criterion than local stability. Both types of stability are simulated with the human driver model of M. Treiber et al. [*Physica A,* Vol. 360, No. 1, 2006, pp. 71–88], which includes all the foregoing features. Several interesting results were found: (*a*) with a suitable anticipation, string stability for reaction times exceeding the safety time gap was obtained (to the authors' knowledge, this result had not yet been achieved for any other car-following model); (*b*) parameter changes that destabilize the model variant with zero reaction time may stabilize the model with finite reaction times, and vice versa; and (*c*) distributed reaction times (every driver has a different reaction time) can stabilize the system compared with the case of drivers with identical reaction times that are equal to the mean.

Modeling of human driving behavior is a controversial topic in traffic science (*1–3*). It is obvious, however, that an essential feature of human (in contrast to automated) drivers is a considerable reaction time, which is a consequence of the physiological aspects of sensing, perceiving, deciding, and performing an action (*4*). This complex reaction time T' is of the order of 1.2 s (*5*). In addition, it varies strongly between different drivers (by age and gender), different stimuli, and different studies [see the review of human perception–brake reaction time studies by Green (*5*)].

Remarkably, in dense (not yet congested) traffic, the modal value in the time gap distribution (which is the most probable value) on Dutch or German freeways is around 0.9 s (*6, 7*), that is, below the average value of the reaction time. This value has to be compared with the linear stability results of simple car-following models, which become unstable if the reaction time exceeds half the value of the time gap (*8, 9*). In such models, the acceleration depends, in general, on the own velocity and the distance and velocity difference to the previous vehicle, which are the input variables of automated driving

Institute for Transport and Economics, Technische Universität Dresden, Andreas-Schubert-Strasse 23, D-01062 Dresden, Germany. Corresponding author: M. Treiber, treiber@vwi.tu-dresden.de.

systems, sometimes called adaptive cruise control (ACC) (*10, 11*). Reaction times are most commonly modeled by introducing a dead time (time delay) T' between the accelerating or braking action of the driver and the input stimuli to which a driver reacts (*8, 12, 13*).

Clearly, human drivers take into account more input variables to overcome the stability limit mentioned earlier. For example, unlike machines, human drivers routinely scan the traffic situation several vehicles ahead and anticipate future traffic situations, which leads, in turn, to an increased stability.

The different stabilizing and destabilizing factors of the driver's behavior and the vehicle dynamics constitute a nonlinear feedback control system and can be visualized in a flow diagram (Figure 1). Instability of traffic flow is caused by the delay that the system needs to respond to a certain action of a controller (*14, 15*). More specifically, the controllers are the drivers; the quantity to be controlled is the velocity of the own vehicle (or the distance to the preceding vehicle); the input stimuli are the observed distances and velocities; and the actions to reach desired velocities or distances consist in accelerating or braking (lane changes are not considered here). The task of following a single vehicle can be modeled by a nonlinear controller containing a gain function (i.e., a car-following model without delay) and a dead-time or delay element. Since only the accelerations can be controlled, the control path contains one or two additional integrative elements. To include anticipation, additional (nonlinear) derivative elements are incorporated into the control path.

To determine the linear local stability, one can apply standard methods of control theory to the linearized system, yielding an upper limit of the reaction time T', which decreases with the sensitivity of the car-following model, that is, how much it accelerates (decelerates) if the actual distance is too large (small). However, it is well known in traffic theory for car-following models with zero reaction time (*16, 3*), and also for macroscopic models (*17*), that small sensitivities (acceleration capabilities) increase the linear string instability if a platoon of several vehicles is considered; that is, the perturbations will amplify while propagating downstream the chain of vehicles. Typically, string or collective stability is a much more restrictive criterion than local stability. The regime of string instability can be further divided into a region of convective instability where perturbations grow but finally are convected out of the system (see, e.g., Figure 2) and a region of absolute instability.

In this contribution, the influence of reaction times, acceleration capabilities, temporal anticipation, and multivehicle look-ahead on the stability of traffic flow is investigated by means of simulation. The discussion includes how these influencing factors change local stability, string stability, and the limits where the traffic flow is accident-free.

The models used for the simulation are presented in the following section. The intelligent driver model (IDM) (*16*) will be used as instantaneous nonlinear controller representing the characteristics
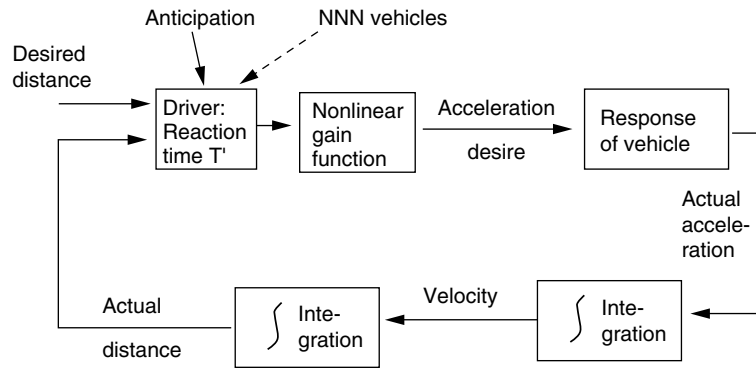
FIGURE 1   Flow diagram of elements of nonlinear feedback loop representing actions of driver and vehicle dynamics.

of automated driving. Its sensitivity is characterized by the acceleration parameter a. The recently proposed human driver model (HDM) (*18*) is based on the IDM and implements the additional human-specific properties (reaction times and anticipations) in a systematic way. Later, results are given and it is shown how each of the factors mentioned earlier influences traffic dynamics. With a suitable anticipation, string stability was obtained for reaction times exceeding the safety time gap, which, to the authors' knowledge, has not yet been done for any other car-following model. Furthermore, it is shown how the different influences of reaction time and acceleration capability on local and string stability lead to an optimal range of the acceleration parameter a rather than a lower limit as proposed in the literature up to now. Finally, for the first time, distributed (i.e., varying) reaction times are simulated.

MICROSCOPIC TRAFFIC MODEL WITH TIME DELAY AND ANTICIPATION

Most microscopic traffic models describe the instantaneous acceleration and deceleration of each individual driver–vehicle unit as a function of the distance and velocity difference to the vehicle in front and of the own velocity (*3*). The subclass of time-continuous microscopic models (car-following models) is of the following general form:

$$\frac{dv_\alpha}{dt} = \alpha^{\text{mic}}\left(s_\alpha, v_\alpha, \Delta v_\alpha\right) \tag{1}$$

where the own velocity v_α, the net distance s_α, and the velocity difference Δv_α to the leading vehicle serve as stimuli determining
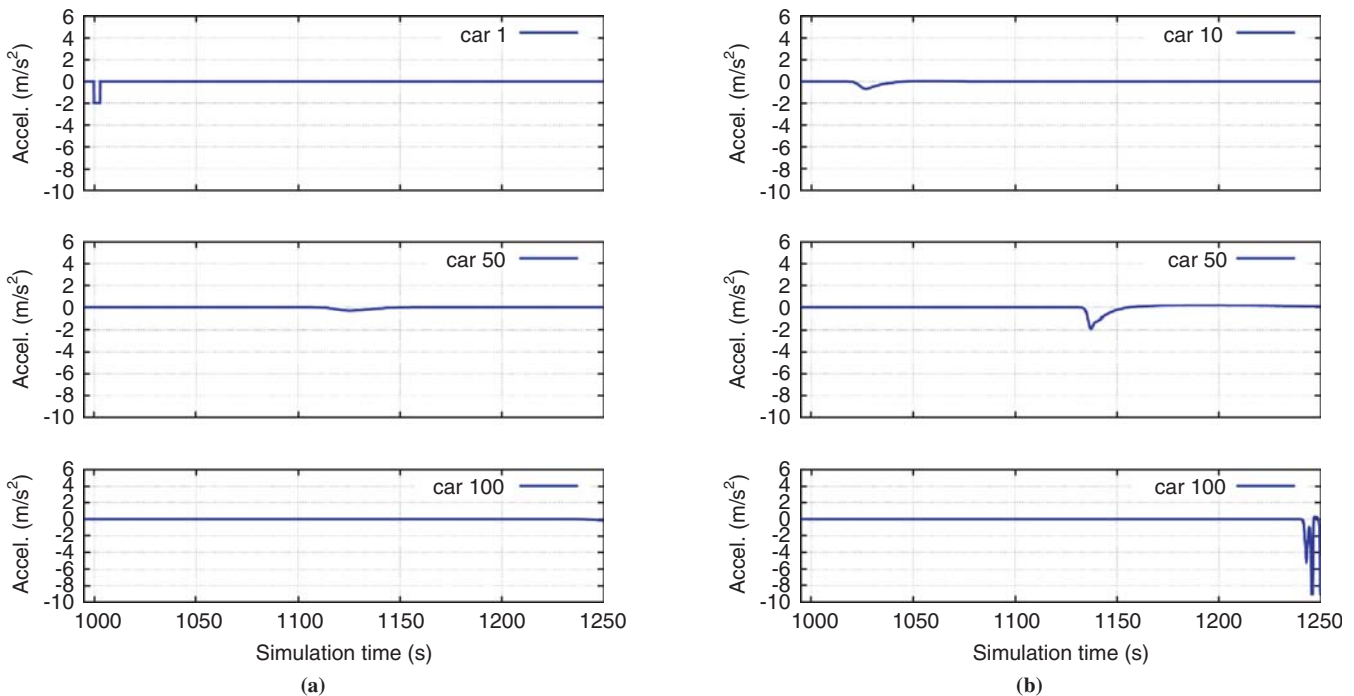

FIGURE 2   Time series of acceleration for selected platoon vehicles for simulations with IDM parameter for maximum acceleration set to (*a*) $a = 1$ m/s^2 and (*b*) $a = 0.3$ m/s^2. In both cases, reaction time is $T' = 0.9$ s, and drivers use temporal anticipation but no spatial anticipation ($n_a = 1$). First vehicle induces perturbation due to braking maneuver at $t = 1,000$ s. For $a = 1$ m/s^2, system is string stable, whereas it is unstable for $a = 0.3$ m/s^2.

the acceleration a^{mic}. This class of basic models is characterized by (*a*) instantaneous reaction, (*b*) reaction only to the immediate predecessor, and (*c*) infinitely exact estimating capabilities of drivers regarding the input stimuli *s, v,* and Δv, which also means that there are no fluctuations—that is, drivers react always in the same way to the same stimuli. In some sense, such models describe driving behavior similar to that of ACC systems (*10, 11*).

In the context of control theory, acceleration is the action to bring (*a*) the own velocity v_α toward the desired velocity v_0 if there is no obstruction from other vehicles, and to the velocity $v_{\alpha-1}$ of the predecessor otherwise, and (*b*) the observed distance s_a toward the equilibrium distance $s_e(v_{\alpha-1})$. Of course, this condition is only relevant in case of obstruction. For models of the form in Equation 1, the equilibrium distance function $s_e(v)$ is given by

$$a^{mic} = (s_e, v, 0) = 0 \tag{2}$$

In general, the control function a^{mic} is strongly nonlinear, and there is a smooth transition from the control targets for unobstructed traffic to that of obstructed traffic. Obstructed traffic (i.e., when it is not possible to drive at the desired velocity) does not necessarily mean congested traffic.

In the following, the IDM (*16*) is introduced, which is a simple car-following model with intuitive parameters. Furthermore, three aspects of human driving behavior are presented: finite reaction times, temporal anticipation, and spatial anticipation (looking several vehicles ahead). These extensions are formulated in a systematic way and apply to all underlying models of the form in Equation 1 (*18*).

Intelligent Driver Model

The IDM acceleration of each vehicle α is a continuous function of the velocity v_α, the net distance gap s_α, and the velocity difference (approaching rate) Δv_α to the leading vehicle:

$$\frac{dv_\alpha}{dt} = a\left[1 - \left(\frac{v_\alpha}{v_0}\right)^4 - \left(\frac{s^*(v_\alpha, \Delta v_\alpha)}{s_\alpha}\right)^2\right] \tag{3}$$

The IDM acceleration consists of a free acceleration $\dot{v}^{free} = a[1 - (v/v_0)^4]$ (with $\dot{v}$ indicating the time derivative) for approaching the desired velocity v_0 with an acceleration slightly below *a* and the braking interaction $\dot{v}^{int} = -a(s^*/s)^2$, where the actual gap s_α is compared with the desired minimum gap:

$$s^*(v, \Delta v) = s_0 + vT + \frac{v\Delta v}{2\sqrt{ab}} \tag{4}$$

which is specified by the sum of the minimum distance s_0, the velocity-dependent safety distance vT corresponding to the time gap *T,* and a dynamic part. The dynamic part implements an accident-free intelligent braking strategy that, in nearly all situations, limits braking decelerations to the comfortable deceleration *b.* It should be noted that all five IDM parameters have an intuitive meaning. The parameters used henceforth (unless stated otherwise) are shown in Table 1. By an appropriate scaling of space and time, the number of parameters can be reduced from five to three.

The IDM was calibrated to empirical data of several German freeways (*16*). On a more microscopic level, the IDM was tested together with other microscopic models (*19*). Although all models showed large residual errors, the IDM was one of the best. Furthermore, with

TABLE 1   IDM Parameters Used

Parameter	Value
Desired velocity v_0	120 km/h
Safety time gap T	1.5 s
Jam distance s_0	2 m
Maximum acceleration a	2.0 m/s²
Desired deceleration b	2.0 m/s²

NOTE: These values were used in this paper unless it is stated otherwise; IDM is used together with explicit reaction time T', temporal anticipation, and spatial anticipation. Vehicle length = 5 m. Maximum braking deceleration is restricted to 9 m/s² as physical limit on dry roads.

the same parameters as those in Table 1 (apart from obvious changes for the desired velocity), both the simulated acceleration behavior from a standstill and the deceleration behavior to a standstill were remarkably close to empirical observations (*20, 21*).

Finite Reaction Time

A reaction time T' is implemented simply by evaluating the right-hand side of Equation 1 at time $t - T'$. If T' is not a multiple of the update time interval, a linear interpolation is proposed according to

$$x(t - T') = \beta x_{t-n-1} + (1 - \beta)x_{t-n} \tag{5}$$

where *x* denotes any quantity on the right-hand side of Equation 1, such as s_α, v_α, or Δv_α; and x_{t-n} denotes this quantity taken *n* time steps before the actual step. Here, *n* is the integer part of T'/t, and the weight factor of the linear interpolation is given by $\beta = T'/t - n$. It must be emphasized that all input stimuli s_α, v_α, and Δv_α are evaluated at the delayed time.

The reaction time T' is sometimes set equal to the safety time gap *T.* However, it is essential to distinguish between these times conceptually. Although the time gap *T* is a characteristic parameter of driving style, the reaction time T' is essentially a physiological parameter and, consequently, at most weakly correlated with *T.* It may be pointed out that both the time gap *T* and the reaction time T' are to be distinguished from the numerical update time step *t,* which is sometimes erroneously interpreted as a reaction time as well.

Temporal Anticipation

It will be assumed that drivers are aware of their finite reaction time and anticipate the traffic situation accordingly. Besides anticipating the future distance (*13*), drivers anticipate the future velocity by using constant-acceleration heuristics. The combined effects of a finite reaction time and temporal anticipation lead to the following input variables for the underlying car-following model (Equation 1):

$$\frac{dv_a}{dt} = \dot{v}^{mic}(s'_\alpha, v'_\alpha, \Delta v'_\alpha) \tag{6}$$

with

$$s'_\alpha(t) = [s_\alpha - T'\Delta v_\alpha]_{t-T'} \tag{7}$$

$$v'_\alpha(t) = \left[v_\alpha + T' \dot{v}_\alpha \right]_{t-T'} \tag{8}$$

and

$$\Delta v'_\alpha(t) = \Delta v_\alpha(t - T') \tag{9}$$

In Equation 8 the time delay occurs in the acceleration $\dot{v}$ as the highest derivative; that is, the linearized model is of the neutral type. The constant-acceleration heuristics were not applied for anticipation of the future velocity difference, or the future distance, since the accelerations of other vehicles cannot be estimated reliably by human drivers. Instead, the simpler constant-velocity heuristics were applied for these cases. It should be noted that the proposed heuristics are parameter-free.

These anticipative terms include derivative quantities (the accelerations) and velocity differences. In the framework of control theory, they act as nonlinear derivative elements in the control path.

Spatial Anticipation for Several Vehicles Ahead

Now the acceleration of the underlying microscopic model is split into a single-vehicle acceleration on a nearly empty road depending on the considered vehicle α only and a braking deceleration taking into account the vehicle–vehicle interaction with the preceding vehicle:

$$\dot{v}^{mic}(s_\alpha, v_\alpha, \Delta v_\alpha) := \dot{v}^{free}_\alpha + \dot{v}^{int}(s_\alpha, v_\alpha, \Delta v_\alpha) \tag{10}$$

This splitting up is motivated by the concept of a social force model, which underlies the IDM and the HDM. In this concept there are several forces, such as a driving force to accelerate to the desired velocity and repulsive forces caused by the front vehicles (18). Next, the reaction to several vehicles ahead is modeled just by summing the corresponding vehicle–vehicle pair interactions $\dot{v}^{int}_\beta$ from vehicle β to vehicle α for the n_a nearest preceding vehicles β:

$$\frac{dv_\alpha}{dt} = \dot{v}^{free}_\alpha + \sum_{\beta=\alpha-n_a}^{\alpha-1} \dot{v}^{int}_{\alpha\beta} \tag{11}$$

where all distances, velocities, and velocity differences on the right-hand side are given by Equations 7 through 9. Each pair interaction between vehicle α and vehicle β is specified by

$$\dot{v}^{int}_{\alpha\beta} = \dot{v}\left(s_{\alpha\beta}, v_\alpha, v_\alpha - v_\beta\right) \tag{12}$$

where the sum of all net gaps between vehicles α and β is

$$s_{\alpha\beta} = \sum_{j=\beta+1}^{\alpha} s_j \tag{13}$$

For the IDM, there exists a closed-form solution of the multianticipative equilibrium distance as a function of the velocity. It should be noted that in the limiting case of anticipation to arbitrary many vehicles, $\lim_{n_a \to \infty} \gamma(n_a) = \pi/\sqrt{6} = 1.283$ is obtained for the IDM. This result means that the combined effects of all non-nearest-neighbor interactions would lead to an increase of the equilibrium distance by just about 28% (18).

In summary, the HDM consists of all extensions of the underlying car-following model just described. The HDM was tested against empirical 1-min data for German freeways (18), and it was found that the model described the observed spatiotemporal structures of congested traffic. Particularly, the transitions between free and congested

traffic were smoother than those in the IDM, in agreement with the empirical results.

MICROSCOPIC TRAFFIC SIMULATIONS OF VEHICLE PLATOONS

String stability is investigated by simulating a platoon of vehicles following an externally controlled lead vehicle. As initial conditions, the platoon is assumed to be in equilibrium; that is, the initial velocities of all platoon vehicles are equal to v_{lead} and the gaps are equal to $s_e(v_{lead})$ (Equation 2), so that the initial model accelerations are equal to zero.

The externally controlled vehicle drives at $v_{lead} = 25$ m/s for the first 1,000 s before it decelerates with -2 m/s^2 for 3 s, which is a realistic scenario in daily traffic. This braking maneuver reduces the velocity to $v_{lead} = 19$ m/s, which is kept constant until the simulation ends at $t = 2,500$ s. The braking maneuver serves as the perturbation for all simulations throughout this paper. It should be noted that the nonlinear dynamics resulting from this finite perturbation can no longer be handled by linearization.

In all simulations, an explicit integration scheme was used assuming constant accelerations between each update time interval Δt according to

$$v_\alpha(t + \Delta t) = v_\alpha(t) + \dot{v}_\alpha(t)\Delta t,$$

$$x_\alpha(t + \Delta t) = x_\alpha(t) + v_\alpha(t)\Delta t + \frac{1}{2}\dot{v}_\alpha(t)(\Delta t)^2 \tag{14}$$

The update time interval is set to $\Delta t = 0.1$ s. The IDM parameters given in Table 1 are used unless stated otherwise. If n_a is larger than the number of preceding vehicles (which can happen for the first vehicles of the platoon), n_a is reduced accordingly. Furthermore, the maximum braking deceleration is restricted to 9 m/s^2, which is the physical limit on dry roads.

Stability Boundaries for Platoon of Vehicles

Three stability regimes are distinguished: (a) string stability, that is, all perturbations introduced by the deceleration of the lead vehicles are damped away; (b) an oscillatory regime, in which perturbations increase but do not lead to collisions; and (c) an instability with accidents. The condition for a simulation to be in the crash regime (c) is fulfilled if there is some time t and some vehicle α so that $s_\alpha(t) < 0$. The condition for string stability is fulfilled if $|\dot{v}_\alpha(t)| < 3$ m/s^2 at all times (including the period in which the leading vehicle decelerates) and for all vehicles. In addition, string stability requires that for sufficiently long times after the braking maneuver, the accelerations of all vehicles converge to zero. Finally, if neither the conditions for the crash regime nor those for the stable regime are fulfilled, the simulation result is attributed to the oscillatory regime.

Figure 3 shows the three stability regimes as a function of the reaction time T' and the platoon size n for the following simulation scenarios:

1. The first scenario with neither spatial anticipation ($n_a = 1$) nor temporal anticipation serves as reference. This case corresponds to the conventional IDM car-following model with finite reaction time. A platoon of 100 vehicles is stable for reaction times of up to $T'_{c1} = 0.9$ s. Test runs with larger platoon sizes (up to 1,000 vehicles) did not result
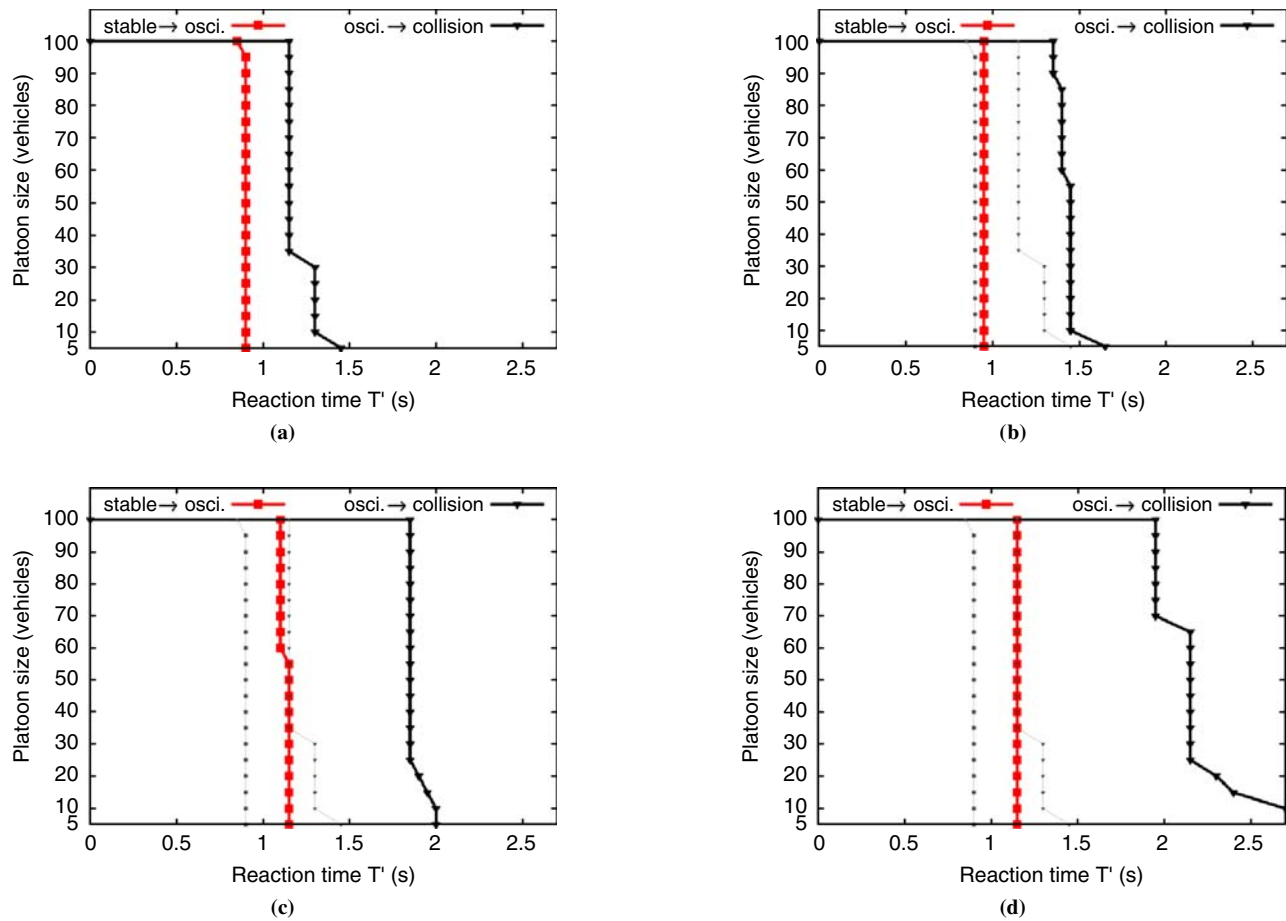
FIGURE 3 String stability regimes of platoon of identical vehicles as function of platoon size and reaction time T' for Scenarios 1 through 4: (a) Scenario 1, assuming conventional follow-the-leader behavior ($n_a = 1$) without temporal anticipation; (b) Scenario 2, with temporal anticipation ($n_a = 1$); (c) Scenario 3, reaction to $n_a = 4$ vehicles without temporal anticipation; and (d) Scenario 4, reaction to $n_a = 4$ vehicles with temporal anticipation.

in different thresholds, suggesting that stability for a platoon size of 100 essentially means string stability for arbitrarily large platoon sizes. For reaction times $T' > T'_{c2} = 1.15$ s, the collective instability leads to accidents, at least when the braking deceleration is limited to 9 m/s².

2. The second scenario extends the reference scenario by implementing the parameter-free temporal anticipation. Although the stability limit, $T'_{c1} = 0.95$ s, is only slightly increased with respect to Scenario 1; the collision limit $T'_{c2} = 1.4$ s is increased significantly.

3. The third simulation scenario implements the spatial anticipation by looking $n_a = 4$ vehicles ahead as extension compared with the reference case $n_a = 1$. This spatial anticipation increases the stability and shifts both boundaries, T'_{c1} and T'_{c2}, to significantly higher values.

4. The fourth scenario combines temporal and spatial anticipation ($n_a = 4$), which leads to the most stable system. In particular, the second boundary is shifted to values of $T'_{c2} \geq 2$ s. Remarkably, the simulation shows that with a suitable anticipation, collision-free traffic could be obtained for reaction times exceeding the safety time gap of $T = 1.5$ s. Further increasing the number of anticipated vehicles n_a does not change the thresholds significantly.

In Figure 3*b–d,* the first scenario of Figure 3*a* is plotted with light dotted lines for purposes of comparison. The externally controlled first

vehicle induced a finite perturbation. In the stable phase, all perturbations are damped away. In the oscillatory regime, the perturbations increase, but do not lead to collision.

So far, constant and identical reaction times $T'_\alpha = T'$ have been assumed for all vehicles α in the simulation. Since human reaction time varies strongly depending on the concrete situation and between different persons (5), the role of distributed reaction times—that is, every driver has a different reaction time T'_α with the mean value $\langle T'_\alpha \rangle = T'$—was also investigated. To this end, the concept was generalized of linear interpolation of Equation 5 to individual delays for each driver–vehicle unit α.

Figure 4 shows the results for several simulation runs for the reference scenario (Scenario 1) without anticipation and Scenario 4 with temporal and spatial anticipation. The reaction time was uniformly distributed within a range of ±30% around the mean value. Interestingly, the phase boundary T'_{c1} between the stable and oscillatory regime is almost not affected by the variation of the reaction time. The phase boundary T'_{c2} for the fourth scenario is even slightly shifted toward higher stability for platoon sizes of $n \geq 70$ vehicles. However, the critical value T'_{c1} is slightly reduced when nonidentical reaction times are involved. The light dotted lines display the phase boundaries for identical reaction times. The variation of the reaction times leads to a remarkably unchanged stability boundary T'_{c1}
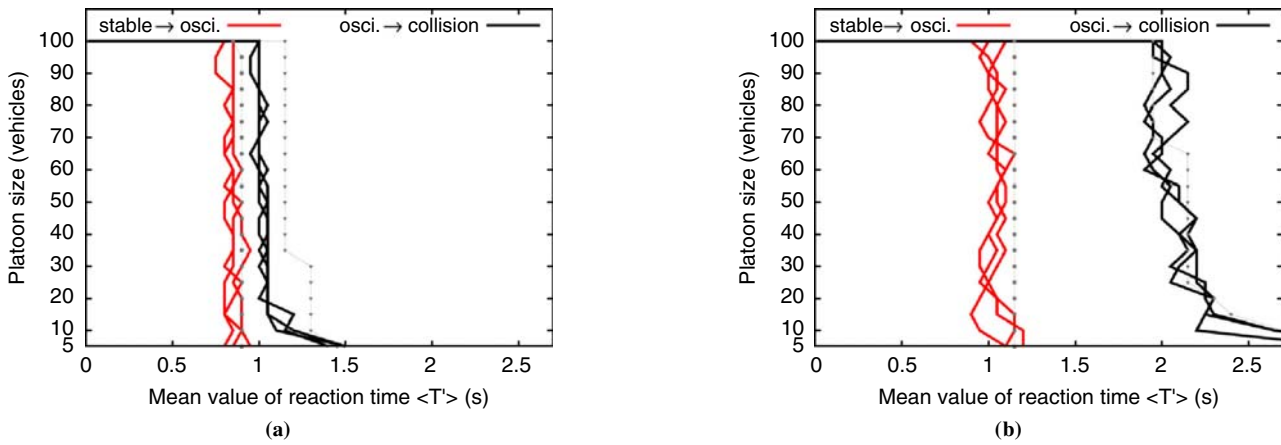
FIGURE 4   String stability regimes of platoon of vehicles α with different individual reaction times for three simulation runs with different random seeds; reaction time T'_α was distributed uniformly within 30% around mean value $\langle T'_\alpha \rangle = T'$: (a) Scenario 1, with neither temporal nor spatial anticipation, and (b) Scenario 4, with temporal and spatial anticipation ($n_a = 4$).

between the stable and oscillating regimes. The critical boundary T'_{c2} is even slightly increased for some platoons (see Figure 4b).

In summary, distributed reaction times have a remarkably low influence on the stability of traffic flow. In particular, the expected stability increase by destructive interference of the different eigenfrequencies of the observations was not observed.

Role of Vehicle Acceleration

As mentioned in the introduction, there are two different sources of instability for traffic flow: the finite reaction time modeled by the HDM parameter T' and finite acceleration capabilities modeled by the IDM parameter a, which gives the maximum acceleration. Clearly, stability always decreases when T' increases. In this subsection, the influence of the acceleration parameter a on the instability mechanisms is investigated and the remarkable result is that stability reaches its maximum for a certain range of values for a (which depends on T'). Traffic flow becomes more unstable if the value of a is higher or lower than this range.

Figure 2a graphs show the time series of the acceleration of some selected vehicles for Scenario 1 with $T' = 0.9$ s and the acceleration parameter changed from 2 m/s² to the approximately optimal value 1 m/s². The system is string stable: the initial perturbation of 2 m/s² dissipates quickly. In the graphs of Figure 2b, the acceleration parameter is lowered from $a = 1$ m/s² to $a = 0.3$ m/s². The effect is as expected (*16, 17*): the initial perturbation decreases for the first few vehicles (the system is locally stable) before it increases again for the next vehicles and finally leads to a traffic breakdown in the neighborhood of Car 100 at a simulated time $t \approx 1,250$ s: the system is string unstable. After the first breakdown, further stop-and-go waves develop (not shown here).

Remarkably, the system becomes unstable as well when the acceleration capability is increased from the reference value $a = 1$ m/s² to $a = 2.5$ m/s² as shown in Figure 5. The instability mechanism, however, is different. For low values of a, the traffic breakdown is initially triggered by a long-wavelength instability, as can be seen in the plots for Cars 10 and 50 of Figure 2b, before additional shorter oscillations appear immediately before the breakdown (Cars 70 and 100). In contrast, the initial instability for high values of a has

its maximum growth rates at shorter frequencies (of about 4 s), which can be seen from Figure 5 for Cars 4 and 50, leading to the first stop-and-go wave, and Cars 50 and 70, leading to the second one. Further stop-and-go waves develop at later times for vehicles further upstream. Interestingly, the period of the resulting stop-and-go waves is about the same for the high-wavelength and low-wavelength mechanisms to
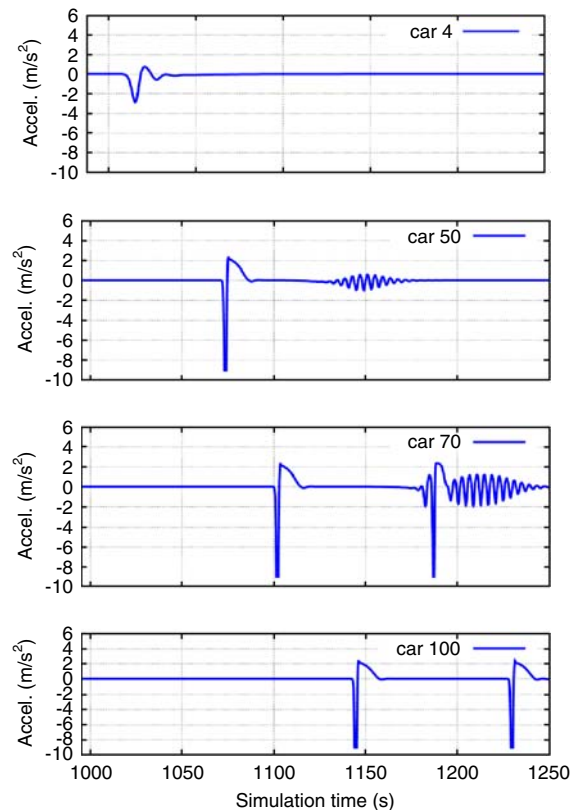

FIGURE 5   Time series of acceleration for same scenario as in Figure 2 but IDM parameter for maximum acceleration is increased to $a = 2.5$ m/s².

instability. Again, the first vehicle induces a perturbation due to the braking maneuver at $t = 1,000$ s (not shown in Figure 5). The increased acceleration parameter a in combination with the delayed reaction causes higher frequencies with periods of about 4 s that finally trigger stop-and-go-waves of a much higher period (about 50 s).

DISCUSSION AND CONCLUSIONS

Two causes for the instability of traffic flow were investigated: the time lag caused by finite accelerations of vehicles and the delay caused by the finite reaction time of drivers. Furthermore, the degree to which drivers may compensate for these delays by looking several vehicles ahead and anticipating future traffic situations was simulated.

Since vehicular traffic flow is a multiparticle system with many degrees of freedom, two concepts of linear stability have to be considered: local stability of a car following a leader that drives at constant velocity and string or collective stability of a platoon of several vehicles following each other. Typically, string stability is a much more restrictive criterion than local stability.

The main results are as follows:

1. By means of simulation, string stability boundaries were determined as a function of reaction time T' for a variable platoon size of vehicles. With suitable spatial and temporal anticipation, string stability for reaction times near the safety time gap were obtained, which, to date, has not yet been done for any other car-following model.

2. When the maximum acceleration capability was varied, the remarkable result that stability reaches its maximum for a certain range of values for a (which depends on the reaction time T') was determined. Traffic flow becomes more unstable if the value of the maximum acceleration is higher or lower than this value. This principle can be understood by the interplay between the two mechanisms to instabilities: if the values of T' and a are both comparatively high, the ratio between the reaction time and the time scale $\tau \approx v_0/a$ of velocity changes is high, leading to instabilities on the level of individual vehicles. Conversely, for low values of a, the lag time scale τ itself leads to the well-known collective instabilities already observed for zero reaction time.

3. Distributed reaction times (i.e., every driver has a different reaction time) can stabilize the system compared with the situation in which drivers have identical reaction times that are equal to the mean. Generally, however, the effect introduced by the heterogeneity among drivers is small.

Whether these results are robust with respect to parameter changes was checked and no qualitative difference for other parameter sets within a reasonable range was found. For example, when the time gap from $T = 1.5$ s to $T = 0.9$ s was changed (see the introduction), the stability thresholds T'_{c1} and T'_{c2} reduce proportionally; that is, T'_{c1} remains typically of the order of or slightly below T, whereas $T'_{c2} > T$. Preliminary results show that the findings are also robust when the HDM is applied to other car-following models.

ACKNOWLEDGMENTS

REFERENCES

1. Brackstone, M., and M. McDonald. Car-Following: A Historical Review. *Transportation Research F,* Vol. 2, 1999, pp. 181–196.
2. Holland, E. A Generalised Stability Criterion for Motorway Traffic. *Transportation Research B,* Vol. 32, 1998, pp. 141–154.
3. Helbing, D. Traffic and Related Self-Driven Many-Particle Systems. *Reviews of Modern Physics,* Vol. 73, 2001, pp. 1067–1141.
4. Shiffrin, R., and W. Schneider. Controlled and Automatic Human Information Processing, II: Perceptual Learning, Automatic Attending, and a General Theory. *Psychological Review,* Vol. 84, 1977, pp. 127–190.
5. Green, M. How Long Does It Take to Stop? Methodological Analysis of Driver Perception–Brake Times. *Transportation Human Factors,* Vol. 2, 2000, pp. 195–216.
6. Tilch, B., and D. Helbing. Evaluation of Single Vehicle Data in Dependence of the Vehicle-Type, Lane, and Site. In *Traffic and Granular Flow '99* (D. Helbing, H. Herrmann, M. Schreckenberg, and D. Wolf, eds.), Springer, Berlin, 2000, pp. 333–338.
7. Knospe, W., L. Santen, A. Schadschneider, and M. Schreckenberg. Single-Vehicle Data of Highway Traffic: Microscopic Description of Traffic Phases. *Physical Review E,* Vol. 65, 2002, p. 056133.
8. Newell, G. Nonlinear Effects in the Dynamics of Car Following. *Operations Research,* Vol. 9, 1961, p. 209.
9. Bando, M., K. Hasebe, A. Nakayama, A. Shibata, and Y. Sugiyama. Dynamical Model of Traffic Congestion and Numerical Simulation. *Physical Review E,* Vol. 51, 1995, pp. 1035–1042.
10. Kesting, A., M. Treiber, M. Schönhof, and D. Helbing. Extending Adaptive Cruise Control (ACC) Toward Adaptive Driving Strategies. In *Transportation Research Record: Journal of the Transportation Research Board, No. 2000,* Transportation Research Board of the National Academies, Washington, D.C., 2007, pp. 16–24.
11. Kesting, A., M. Treiber, M. Schönhof, F. Kranke, and D. Helbing. Jam-Avoiding Adaptive Cruise Control (ACC) and Its Impact on Traffic Dynamics. In *Traffic and Granular Flow '05,* Springer, Berlin, 2007, pp. 633–643 (e-print physics/0601096).
12. Bando, M., K. Hasebe, K. Nakanishi, and A. Nakayama. Analysis of Optimal Velocity Model with Explicit Delay. *Physical Review E,* Vol. 58, 1998, p. 5429.
13. Davis, L. Modifications of the Optimal Velocity Traffic Model to Include Delay due to Driver Reaction Time. *Physica A,* Vol. 319, 2002, p. 557.
14. Brogan, W. L. *Modern Control Theory.* Prentice Hall, Upper Saddle River, N.J., 1991.
15. Isidori, A. *Nonlinear Control Systems.* Springer, New York, 1995.
16. Treiber, M., A. Hennecke, and D. Helbing. Congested Traffic States in Empirical Observations and Microscopic Simulations. *Physical Review E,* Vol. 62, 2000, pp. 1805–1824.
17. Treiber, M., A. Hennecke, and D. Helbing. Derivation, Properties, and Simulation of a Gas-Kinetic-Based, Non-Local Traffic Model. *Physical Review E,* Vol. 59, 1999, pp. 239–253.
18. Treiber, M., A. Kesting, and D. Helbing. Delays, Inaccuracies and Anticipation in Microscopic Traffic Models. *Physica A,* Vol. 360, 2006, pp. 71–88.
19. Brockfeld, E., R. D. Kühne, and P. Wagner. Calibration and Validation of Microscopic Traffic Flow Models. In *Transportation Research Record: Journal of the Transportation Research Board, No. 1876,* Transportation Research Board of the National Academies, Washington, D.C., 2004, pp. 62–70.
20. Wang, J., K. K. Dixon, H. Li, and J. Ogle. Normal Acceleration Behavior of Passenger Vehicles Starting from Rest at All-Way Stop-Controlled Intersections. In *Transportation Research Record: Journal of the Transportation Research Board, No. 1883,* Transportation Research Board of the National Academies, Washington, D.C., 2004, pp. 158–166.
21. Wang, J., K. K. Dixon, H. Li, and J. Ogle. Normal Deceleration Behavior of Passenger Vehicles at Stop Sign–Controlled Intersections Evaluated with In-Vehicle Global Positioning System Data. In *Transportation Research Record: Journal of the Transportation Research Board, No. 1937,* Transportation Research Board of the National Academies, Washington, D.C., 2005, pp. 120–127.